A Forward Displacement Analysis of a Class of Stewart Platforms

M. Griffis

Research Assistant

J. Duffy

Graduate Research Professor in Mechanical Engineering

Center for Intelligent Machines and Robotics

University of Florida

Gainesville, FL 32611

USA

January 1989

ABSTRACT

A closed-form forward displacement analysis is performed for a Stewart Platform-type of parallel mechanism, whose six legs meet in a pair-wise fashion at three points in the top and base platforms. The six legs and two platforms of this mechanism together form an octahedron. An eighth degree polynomial in the square of the tan-half-angle that measures the elevation of a triangular face of the octahedron relative to the base triangle is derived. Each of three vertices of the base triangle of the octahedron is modeled by a spherical four-bar mechanism, and the polynomial is obtained by eliminating a pair of tan-half-angular displacements from the displacement equations of the three spherical four-bar mechanisms. The results are verified numerically by performing a reverse displacement analysis and displaying real solutions on a graphics system. It is clear that there are a maximum of eight reflected pairs of real assembly configurations of the octahedral form of the Stewart Platform.

INTRODUCTION

Over the past few years, there has been an ever increasing interest in direct applications of parallel mechanisms to real-world industrial problems. In situations where the needs for accuracy and sturdiness dominate the requirement of a large workspace, parallel mechanisms present themselves as viable alternatives to their serial counterparts. This paper is confined to the forward displacement analysis of Stewart Platform-type parallel mechanisms. In the general sense, each of these mechanisms consists of two platforms that are connected by six prismatic joints acting in-parallel. One of the platforms is defined as the "top platform". It has six degrees-of-freedom relative to the other platform, which is the "base". It is then required to compute all possible locations (positions and orientations) of the top platform measured relative to the base for arbitrary sets of six connecting prismatic leg lengths.

Stewart [1] introduced his platform in 1965 as an aircraft simulator. Since then, many parallel mechanisms containing prismatic joints have been called Stewart Platforms, although Stewart originally suggested only two different arrangements. Hunt [2, 3], Mohamed and Duffy [4], Fichter [5], Sugimoto [6, 7], Rees-Jones [8], and Kerr [9] all suggest use of Stewart Platforms, with various applications ranging from manipulators to force/torque sensors. Reinholtz and Gokhale [10] (as well as Miura, Furuya, and Suzuki [11], and Miura and Furuya [12]) investigated an interesting application in the form of "Variable Geometry Truss Robots (VGT's)". It is apparent that NASA's octahedral VGT is in fact founded on the simplest of the Stewart Platforms.

Much of the research in the literature has devoted extensive effort to the reverse displacement analysis that is inherently simple for parallel mechanisms (viz. it required to compute a set of leg lengths given a desired location of the top platform relative to the base). Few, however, have investigated closed-form forward displacement analyses for

parallel mechanisms. Instead, they depend on purely numerical solutions. Behi [13] investigated a forward displacement analysis of a parallel mechanism that closely resembles a Stewart Platform. Numerically, he was able to find eight solutions. Reinholz and Gokhale [10] used the Newton-Raphson technique to obtain an iterative solution for the forward displacement analysis of a Stewart Platform.

A closed-form forward displacement analysis (as opposed to an iterative one) will yield much important information on the geometry and kinematics of a parallel mechanism. For instance, a closed-form solution for a Stewart Platform will not only yield the exact number of real configurations of the top platform relative to the base for a specified set of leg lengths but also quantify the effects of errors in leg lengths on the position and orientation of the top platform. Futhermore, a forward displacement analysis of a Stewart Platform manipulator will provide a Cartesian controller with necessary feedback information, namely the position and orientation of the top platform relative to the base. This is especially important when the actual position and orientation cannot be directly sensed, and when the manipulator's configuration is determined solely from lengths of the connecting prismatic legs. Near singularities, purely numerical solutions may experience difficulties, since they provide no way to determine changes in closure.

Additionally, in the field of force control, a forward analysis would provide the necessary analytics to enhance the use of a Stewart Platform as a force/torque sensor. A Stewart Platform design that is based on an in-parallel structure lends itself well to static force analysis, particularly when utilizing the theory of screws [8, 9]. The wrench applied to the top platform can be statically equated to the summation of the forces measured along the lines of the six prismatic legs. Thus far, this particular application of the Stewart Platform has depended on relatively "small" leg deflections, resulting in a

"constant" configuration. However, employing a forward displacement analysis provides the analytics to monitor gross deflections of the Stewart Platform and thereby permit one to consider the design of a more compliant force/torque sensor. In other words, a forward analysis will generate the geometry of the lines of the six connecting prismatic legs of the Stewart Platform so that the effects of finite changes in leg lengths can be related to the forces and torques (wrenches) applied to the top platform.

In this paper, a closed-form solution is presented for the forward displacement analysis of a Stewart Platform whose six legs meet in a pair-wise fashion at three points in the top and base platforms. (See Figure 1a.) In terms of solid geometry, this structure is an octahedron having eight triangular faces. (See Figure 1b for a plan view.) In terms of mechanisms, the top platform is supported by six SPS[1] serial chains that act in-parallel. This means that there must be a pair of concentric and independent spherical joints located at each of the vertices on both the top and base platforms. This Stewart Platform arrangement will be refered to in this paper as a "3-3 Stewart Platform".

For the forward displacement analysis, the lengths of the six prismatic joints are given, together with the lengths of the edges of the top and base platforms. In other words, all edges of the octahedron are known. It remains then to find all possible ways to assemble the eight triangles, such that the edges of each triangle share the correct edges of three adjacent triangles.

In order to solve this forward analysis problem, it was necessary to eliminate a pair of unwanted tan-half-angles from a set of three simultaneous quadratic equations. As far as the authors are aware, the eliminant for this set of equations has not been

---

[1]Here and throughout, the capital letters R, S, and P denote respectively, revolute, spherical, and prismatic kinematic pairs.

In an SPS serial chain, the prismatic joint (P) has an extra degree-of-freedom, a rotation about the line joining the centers of its S pairs. This extra degree-of-freedom in each leg does not affect the gross motion of the top platform.

previously reported in the literature. Sets of equations of this type appear frequently in the kinematic analysis of mechanisms, and hence it is considered that this general eliminant will provide closed-form solutions to a number of other kinematic and geometric problems. The expansion of the eliminant for the 3-3 Stewart Platform yields an eighth degree polynomial in the square of a single tan-half-angle. It follows that there are a maximum of 16 real assembly configurations of this Stewart Platform. Because of the reflections of the mechanism through the base platform, these assembly configurations are grouped pair-wise. Therefore, there are, for a given set of leg lengths, a maximum of eight reflected pairs of real solutions to this forward displacement analysis.

Pairs of concentric spherical joints may well present design problems by causing interference between cointersecting connecting legs. It is thus of great importance to eliminate, as far as possible, the use of concentric spherical joints. In this respect, the solution for this 3-3 Stewart Platform is extended by construction to the solution of a 6-3 Stewart Platform with a triangular top and a hexagonal base. (See Figures 2a and 2b.) Each of the six serial chains is still modeled by an SPS sequence of joints. However, each pair of concentric spherical joints on the base platform have now been separated.

THE FORMULATION OF THE FORWARD ANALYSIS PROBLEM

Inherently, the base platform contains three spherical four-bar linkages. (See Figure 3.) Here, the vertices on the base platform are o, p, and q, and the vertices on the top are r, s, and t.[2] In other words, each of the octahedron's vertices that are in the triangular base (o, p, and q) is the center of two concentric spherical joints that connect a pair of legs to the base platform. Four lines radiate from each of these three vertices:

[2]This analysis is also valid when formulated from the top platform, specifically using points r, s, and t.

two are platform legs, and the other two are sides of the triangular base. At each vertex, the four lines form, in a pair-wise fashion, four planes. When a sphere of unit radius is centered at a given vertex, then the four planes through the vertex cut it in four arcs of great circles. (Figure 4 shows q as a representative vertex.) These four arcs of great circles form a spherical quadrilateral that is a skeletal model of a 4R spherical mechanism with mobility one [14, 15, and 16].

A single, generalized spherical four-bar linkage is shown in Figure 5. The four links, the output, coupler, input, and grounded links, are denoted respectively by the angles, α_{12}, α_{23}, α_{34}, and α_{41}.[3] For this generalized spherical four-bar linkage, the input angle is denoted by θ_4, and the output angle by θ_1.

Refering back to Figure 3, one can associate three spherical four-bar linkages with the generalized spherical four-bar linkage of Figure 5. The grounded links for these spherical four-bar linkages are all attached to the base platform. They are, in fact, the three interior angles of the triangle that forms the base platform. The coupler links for these spherical four-bar linkages are angles contained in the triangles ors, pst, and qrt. The input and output links are six angles taken from the three triangles that are known to share edges with the base platform. These are the triangles ops, pqt, and qor.

Summarizing, twelve link angles are required to define these three spherical four-bar mechanisms, and they are listed in Table 1.

Table 1. Link angles that define the three spherical four-bar linkages.

Origin	o	p	q
Output, α_{12}	$\angle$qor	$\angle$ops	$\angle$pqt
Coupler, α_{23}	$\angle$ros	$\angle$spt	$\angle$tqr
Input, α_{34}	$\angle$sop	$\angle$tpq	$\angle$rqo
Ground, α_{41}	$\angle$poq	$\angle$qpo	$\angle$oqp.

[3]The notation used here was employed by Duffy [16].

The cosines of these 12 angles are obtained via the cosine law for an interior angle of a planar triangle. To adequately determine these link angles, it is necessary to account for the signs of sines of these 12 angles. Firstly, the signs of the sines of the grounded links are considered as known, since the location of the points o, p, and q are known. Secondly, it will be seen that the input-output relation for the generalized spherical four-bar linkage is not a function of the sine of the coupler link. This obviates the need for the signs of the sines of the coupler links.

Lastly, the signs of the sines of the pairs of input and output links are not known. Following Gilmartin and Duffy [17], this does not present a problem for a single four-bar spherical mechanism. However, adjacent input and output links of the three spherical four-bar mechanisms must be consistent in the signs of the sines. For instance, the sines of the angles $\angle$sop and $\angle$ops must either be both positive or both negative. The same must be true for the pairs of angles ($\angle$tpq, $\angle$pqt) and ($\angle$rqo, $\angle$qor). It will be shown that selecting any of these eight combinations will yield identical assembly configurations.

The input angle of one spherical four-bar is precisely the output angle for its adjacent one. (Refer to Figure 3.) For instance, the input angle for the spherical four-bar linkage at o is labeled θ_y. This angle, which is also the output angle for the spherical four-bar linkage at p, is the angular elevation of the triangle ops relative to the base platform. Analogously, θ_z and θ_x measure the elevations of triangles pqt and qor relative to the base. The angles θ_x, θ_y, and θ_z are defined as "fold angles". For the three spherical four-bar linkages, these fold angles can be related to θ_1 and θ_4 using Table 2.

Table 2. The input and output angles for the three spherical four-bar linkages.

Origin	o	p	q
Output, θ_1	θ_x	θ_y	θ_z
Input, θ_4	θ_y	θ_z	θ_x.

Given 12 edge lengths for an octahedron that defines a 3-3 Stewart Platform, applications of a cosine law for interior angles of triangles determine the 12 angles that define the three spherical four-bar linkages. Once these three spherical mechanisms of mobility one are defined, it remains to determine all possible sets of fold angles, namely θ_X, θ_Y, and θ_Z. For each triplet of fold angles, there is a unique assembly configuration of the 3-3 Stewart Platform.

THE SOLUTION OF THE FORWARD ANALYSIS PROBLEM

It has been established that it is necessary to compute the angles θ_X, θ_Y, and θ_Z in order to determine the position and orientation of the top platform relative to the base platform of the Stewart Platform of Figure 3. These three angles are related through the input-output relations for the three spherical four-bar linkages described above.

For the generalized spherical four-bar linkage of Figure 5, the relationship between the input angle (θ_4) and the output angle (θ_1) is dependent on the output, coupler, input, and grounded links, which are respectively, α_{12}, α_{23}, α_{34}, and α_{41}. This relationship is

$$\begin{aligned}(s_{12}\, c_{41}\, s_{34})\, c_4 c_1 + (s_{12}\, s_{41}\, c_{34})\, c_1 + (s_{41}\, s_{34}\, c_{12})\, c_4 \\ - (s_{12}\, s_{34})\, s_4 s_1 + c_{23} - c_{12}\, c_{41}\, c_{34} = 0,\end{aligned} \tag{1}$$

where $s_{12} = \sin(\alpha_{12})$, ..., $c_4 = \cos(\theta_4)$. Clearly, this input-output relationship does not contain the sine of the coupler link, α_{23}.

It is convenient to introduce the tan-half-angle relationships for θ_4 and θ_1:

$$c_j = \frac{1 - w_j^2}{1 + w_j^2} \quad \text{and} \quad s_j = \frac{2\, w_j}{1 + w_j^2} \text{ , where } \quad w_j = \tan\left(\frac{\theta_j}{2}\right) \text{ for } j = 1 \text{ and } 4.$$

Equation (1) then assumes the form

$$A\, w_1^2\, w_4^2 + B\, w_1^2 + C\, w_4^2 + D\, w_1\, w_4 + E = 0, \tag{2}$$

where the five coefficients for a single input-output relation are

$$A = s_{12}\, c_{41}\, s_{34} - s_{12}\, s_{41}\, c_{34} - s_{41}\, s_{34}\, c_{12} + c_{23} - c_{12}\, c_{41}\, c_{34}$$

$$B = -\, s_{12}\, c_{41}\, s_{34} - s_{12}\, s_{41}\, c_{34} + s_{41}\, s_{34}\, c_{12} + c_{23} - c_{12}\, c_{41}\, c_{34}$$

$$C = -\, s_{12}\, c_{41}\, s_{34} + s_{12}\, s_{41}\, c_{34} - s_{41}\, s_{34}\, c_{12} + c_{23} - c_{12}\, c_{41}\, c_{34}$$

$$D = -\, 4\, s_{12}\, s_{34}$$

$$E = s_{12}\, c_{41}\, s_{34} + s_{12}\, s_{41}\, c_{34} + s_{41}\, s_{34}\, c_{12} + c_{23} - c_{12}\, c_{41}\, c_{34}\,.$$

By an exchange of variables, Equation (2) can be used to obtain the input-output equations for the three spherical four-bars on the base platform. Using the "o" columns of Tables 1 and 2, Equation (2) can be expressed in the form

$$A_1\, x^2\, y^2 + B_1\, x^2 + C_1\, y^2 + D_1\, x\, y + E_1 = 0. \tag{3}$$

Here, the five coefficients A_1, ..., E_1 replace A, ..., E, where α_{12}, ..., α_{34} are given by $\angle$qor, ..., $\angle$poq in the "o" column of Table 1. Also, from the "o" column of Table 2, the relations $x = \tan\left(\frac{\theta_x}{2}\right)$ and $y = \tan\left(\frac{\theta_y}{2}\right)$ replace w_1 and w_4. Analogously, the following

two equations are obtained by respectively using the "p" and "q" columns of Tables 1 and 2.

$$A_2\, z^2\, x^2 + B_2\, z^2 + C_2\, x^2 + D_2\, z\, x + E_2 = 0 \tag{4}$$

$$A_3\, y^2\, z^2 + B_3\, y^2 + C_3\, z^2 + D_3\, y\, z + E_3 = 0. \tag{5}$$

Now, the coefficients A_2, ..., E_2 and A_3, ..., E_3 replace A, ..., E of Equation (2), and the third tan-half-angle relation $z = \tan\left(\frac{\theta_z}{2}\right)$ is introduced.

It is interesting to note that when all edges of the octahedron are equal, then all of the triangular faces are equilateral, and all four links of each spherical four-bar mechanism are 60°. Equations (3), (4), and (5) then reduce to $xy=zx=yz=1/2$. This yields the unique solution $\theta_x=\theta_y=\theta_z=70.53°$ for the regular octahedron, which is one of the Platonic solids.

For the general case, it remains to eliminate y and z from (3), (4), and (5) and obtain a polynomial in x. It is convenient to re-write (3) and (4) in the condensed form:

$$a_1\, y^2 + 2\, b_1\, y + c_1 = 0 \tag{6}$$

$$a_2\, z^2 + 2\, b_2\, z + c_2 = 0, \tag{7}$$

where

$$a_1 = A_1\, x^2 + C_1, \qquad b_1 = 0.5\, D_1\, x, \qquad c_1 = B_1\, x^2 + E_1,$$

$$a_2 = A_2\, x^2 + B_2, \qquad b_2 = 0.5\, D_2\, x, \text{ and } \quad c_2 = C_2\, x^2 + E_2.$$

The eliminant, Δ, of (5), (6), and (7) can be expressed in the form

$$\Delta = \alpha^2 - 4\,\beta^2 \rho_1 \rho_2\,, \tag{8}$$

where

$$\begin{aligned}
\alpha = \; & 2\,A_3\,B_3\,a_2\,c_1^2\,c_2 - 4\,A_3\,B_3\,c_1^2\,b_2^2 + 2\,A_3\,C_3\,a_1\,c_1\,c_2^2 - 4\,A_3\,C_3\,c_2^2\,b_1^2 \\
& - 2\,A_3\,E_3\,a_1\,a_2\,c_1\,c_2 + 4\,A_3\,E_3\,a_1\,c_1\,b_2^2 + 4\,A_3\,E_3\,a_2\,c_2\,b_1^2 \\
& - 8\,A_3\,E_3\,b_1^2\,b_2^2 - 2\,A_3\,D_3\,c_1\,c_2\,b_1\,b_2 - 2\,B_3\,C_3\,a_1\,a_2\,c_1\,c_2 \\
& + 4\,B_3\,C_3\,a_1\,c_1\,b_2^2 + 4\,B_3\,C_3\,a_2\,c_2\,b_1^2 - 8\,B_3\,C_3\,b_1^2\,b_2^2 \\
& + 2\,B_3\,E_3\,a_1\,a_2^2\,c_1 - 4\,B_3\,E_3\,a_2^2\,b_1^2 - 2\,B_3\,D_3\,a_2\,c_1\,b_1\,b_2 \\
& + 2\,C_3\,E_3\,a_1^2\,a_2\,c_2 - 4\,C_3\,E_3\,a_1^2\,b_2^2 - 2\,C_3\,D_3\,a_1\,c_2\,b_1\,b_2 \\
& - 2\,D_3\,E_3\,a_1\,a_2\,b_1\,b_2 - D_3^2\,a_1\,a_2\,c_1\,c_2 - A_3^2\,c_1^2\,c_2^2 \\
& - B_3^2\,a_2^2\,c_1^2 - C_3^2\,a_1^2\,c_2^2 - E_3^2\,a_1^2\,a_2^2
\end{aligned}$$

$$\begin{aligned}
\beta = \; & 4\,A_3\,E_3\,b_1\,b_2 + A_3\,D_3\,c_1\,c_2 + D_3\,E_3\,a_1\,a_2 \\
& - 4\,B_3\,C_3\,b_1\,b_2 - B_3\,D_3\,a_2\,c_1 - C_3\,D_3\,a_1\,c_2
\end{aligned}$$

$$\rho_1 = b_1^2 - a_1\,c_1$$

$$\rho_2 = b_2^2 - a_2\,c_2.$$

When Δ vanishes, (5), (6), and (7) have simultaneous solutions in the variables y and z. The equation $\Delta=0$ is an eighth degree polynomial in x^2. It follows that there are 16 solutions for x and a corresponding 16 pairs of solutions for y and z.

The 16 solutions are pair-wise reflections of eight solutions through the base platform. There can be 0, 4, 8, 12, or 16 real solutions. Therefore, there can be 0, 2, 4, 6, or 8 pairs of real, reflected solutions.

NUMERICAL EXAMPLE

Here, a numerical example illustrates 12 real solutions, with six reflected through the base platform. The edges were as follows:

or	os	ps	pt	qt	qr	op	pq	qo	rs	st	tr
17.8	19.8	18	18	17	14.9	12	12	12	6	6	6

Only the ratios are important. The base and top platforms are equilateral triangles. However, the leg lengths produce no further symmetry.

For this example, the following polynomial was obtained via the expansion of the eliminant (Δ=0).

$$\Delta = x^{16} - 13.3... x^{14} + 73.4... x^{12} - 215.5... x^{10} + 368.2... x^{8}$$
$$- 374.1...x^{6} + 220.4...x^{4} - 69.0...x^{2} + 8.8... = 0.$$

This polynomial has the following 16 roots:

$$x = \pm 0.862..., \pm 1.078..., \pm 1.395..., \pm 1.382..., \pm 1.701...\pm 1.922...,$$
$$(0.711... \pm i\ 0.017...), \text{ and } (-0.711... \pm i\ 0.017...).$$

Figure 6 shows six real configurations. There are a corresponding six reflections of these configurations through the base platform. It is interesting to note that five of these six solutions produce concave octahedra. Only the second solution is of the convex form that was depicted in Figure 1. These solutions correspond to the first six positive roots.

In Figure 6, the origin of the coordinate system on the base is o, p lies on the x axis, and q is in the positive xy plane. The origin of the coordinate system on the top is r, s lies on the x axis, and t is in the positive xy plane. Relative to the coordinate system on the base platform, the locations of the points r, s, and t are listed in Table 3. In order to verify these results, a reverse displacement analysis was performed. All 16 solutions, including complex ones, reproduced the correct edge lengths with at least 8 digits of accuracy. Further, it was verified that identical solutions were obtained, whether the signs of the sines of appropriate pairs of input and output links were taken as positive or negative.

EXTENDED APPLICATIONS

Through construction, this same forward displacement analysis is directly applicable to many other parallel mechanisms. For example, when the concentric spherical joints on the base of the 3-3 Stewart Platform are separated but kept in the same plane, the 6-3 Stewart Platform of Figure 2 is obtained. The same forward displacement analysis described in this paper applies to this 6-3 arrangement. Stewart [1] originally proposed the 6-3 arrangement, describing it to be under "linear coordinate control". In his description, the base-end spherical joint of each SPS serial chain was shown as a Hooke joint. Substituting Hooke joints for spherical joints on the base platform would remove the rotatability of any prismatic joint about the line that connected its original spherical joints but would not affect the mobility of the top platform.

Specifically, a 6-3 Stewart Platform can be modeled by a 3-3 Platform by extending the sides of the hexagonal base as shown in Figure 7. The lengths of the edges of the top platform, the locations of points o', p', and q', and the lengths of the six connecting prismatic joints are known. Then, six "virtual" connecting leg lengths ($o'r$,

o's, p's, $p't$, $q't$, and $q'r$) can be uniquely calculated, creating a "virtual" 3-3 Stewart Platform. Therefore, this 6-3 Stewart Platform is geometrically similar to the 3-3 version. This was first noted by Fichter [5]. Furthermore, three pairs of concentric spherical joints have been separated, without increasing the complexity of the mechanism.

ACKNOWLEDGEMENT

The authors would like to thank Lotfi Romdhane, University of Florida, for graphically displaying the numerical results.

REFERENCES

1. Stewart, D., 1965, "A Platform with Six Degrees-of-Freedom," Proc. Inst. Mech. Eng., London, Volume 180, pages 371–386.

2. Hunt, K. H., 1978, Kinematic Geometry of Mechanisms, Oxford University Press, London.

3. Hunt, K. H., 1983, "Structural Kinematics of In-Parallel-Actuated Robot-Arms," Trans. ASME, J. of Mech., Trans., and Auto. in Design, Vol. 105, pages 705–712, ASME Paper No. 82-DET-105.

4. Mohamed, M. G., and Duffy, J., 1985, "A Direct Determination of the Instantaneous Kinematics of Fully Parallel Robotic Manipulators," ASME Journal of Mechanisms, Transmissions, and Automation in Design, Volume 107, pages 226-229, ASME Paper No. 84-DET-114.

5. Fichter, E. F., 1986, "A Stewart Platform-Based Manipulator: General Theory and Practical Construction," Int. J. Robotics Research, Volume 5, No. 2, pages 157–182.

6. Sugimoto, K., 1986, "Kinematic and Dynamic Analysis of Parallel Manipulators by Means of Motor Algebra," ASME Paper No. 86-DET-139.

7. Sugimoto, K., 1988, "Computational Scheme for Dynamic Analysis of Parallel Manipulators," Trends and Developments in Mechanisms, Machines, and Robotics —1988, Volume 3, pages 59-64.

8. Rees-Jones, J., 1987, "Cross Coordinate Control of Robotic Manipulators," Proceedings of the International Workshop on Nuclear Robotic Technologies and Applications, Present and Future, University of Lancaster, UK, June 29—July 1, 1987.

9. Kerr, D. R., 1988, "Analysis, Properties, and Design of a Stewart-Platform Transducer," Trends and Developments in Mechanisms, Machines, and Robotics — 1988, Volume 3, pages 139-146.

10. Reinholz, C., and Gokhale, D., 1987, "Design and Analysis of Variable Geometry Truss Robots," Proceedings of the 9^{th} Annual Applied Mechanisms Conference.

11. Miura, Furuya, and Suzuki, 1984, "Variable Geometry Truss and its Application to Deployable Truss and Space Crane Arm", 35th Congress of the International Astronautical Federation, Lausanne, Switzerland.

12. Miura and Furuya, 1985, "An Adaptive Structure Concept for Future Space Applications", 36th Congress of the International Astronautical Federation, Stockholm.

13. Behi, F., 1988, "Kinematic Analysis for a Six-degree-of-freedom 3-PRPS Parallel Mechanism", IEEE Journal of Robotics and Automation, Volume 4, pages 561-565.

14. Willis, R., 1870, Principles of Mechanisms, Longmans, Green and Co., Ltd., London.

15. Reuleaux. F., 1963. (Translated by A. Kennedy), The Kinematics of Machinery. Dover Pub. Inc., New York.

16. Duffy, J., 1980, Analysis of Mechanisms and Robotic Manipulators, Edward Arnold, London.

17. Gilmartin, M., and Duffy, J., 1972, "Type and Mobility Analysis of the Spherical Four-Link Mechanisms", Inst. Mech. Eng., Mechanisms, pages 90-97.

APPENDIX

The eliminant, Equation (8), of Equations (5), (6), and (7) was obtained by first expressing Equations (6) and (7) in the forms

$$y^2 = \frac{-(2\,b_1\,y + c_1)}{a_1} \quad \text{and} \quad z^2 = \frac{-(2\,b_2\,z + c_2)}{a_2}\,.$$

These forms of Equations (6) and (7) were substituted into Equation (5) to obtain the following bi-linear expression:

$$a_3\,y\,z + b_3\,y + c_3\,z + d_3 = 0, \tag{i}$$

where $a_3 = 4\,A_3\,b_1\,b_2 + D_3\,a_1\,a_2\,,$

$b_3 = 2\,A_3\,b_1\,c_2 - 2\,B_3\,a_2\,b_1\,,$

$c_3 = 2\,A_3\,b_2\,c_1 - 2\,C_3\,a_1\,b_2\,,$ and

$d_3 = A_3\,c_1\,c_2 + E_3\,a_1\,a_2 - B_3\,a_2\,c_1 - C_3\,a_1\,c_2\,.$

Following this, the solutions to Equations (6) and (7) were expressed in the forms

$$y = \frac{-\,b_1 \pm \sqrt{\rho_1}}{a_1} \quad \text{and} \quad z = \frac{-\,b_2 \pm \sqrt{\rho_2}}{a_2}\,, \tag{ii}$$

where $\rho_i = b_i^2 - a_i\,c_i$. Substituting (ii) into (i) and re-arranging yielded the expression

$$a_3\,\sqrt{\rho_1}\,\sqrt{\rho_2} + \left(d_3\,a_1\,a_2 - c_3\,a_1\,b_2 - b_3\,a_2\,b_1 + a_3\,b_1\,b_2\right) =$$

$$\left(a_3\,b_2 - b_3\,a_2\right)\left(\pm\,\sqrt{\rho_1}\right) + \left(a_3\,b_1 - c_3\,a_1\right)\left(\pm\,\sqrt{\rho_2}\right). \tag{iii}$$

Squaring both sides of Equation (iii), re-arranging, and dividing throughout by the extraneous factors $a_1\,a_2$ yielded the expression

$$2\,\beta\,\sqrt{\rho_1}\,\sqrt{\rho_2} = \alpha\,, \tag{iv}$$

where

$$\alpha = 2\,(a_3\,b_3\,b_2\,c_1 + a_3\,c_3\,b_1\,c_2 + b_3\,d_3\,a_2\,b_1 + c_3\,d_3\,a_1\,b_2)$$

$$- (a_3^2\,c_1\,c_2 + b_3^2\,a_2\,c_1 + c_3^2\,a_1\,c_2 + d_3^2\,a_1\,a_2)$$

$$- 2\,b_1\,b_2\,(a_3\,d_3 + b_3\,c_3)$$

and

$$\beta = a_3\,d_3 - b_3\,c_3\,.$$

The final form of Equation (8) was obtained by squaring (iv), moving the resulting left-hand side to the right-hand side, and back-substituting the expressions for a_3, b_3, c_3, and d_3 given in Equation (i).

Table 3. The results of the forward displacement analysis for the numerical example. (Only the eight upper reflections are given. Figure 6 illustrates the first six data.)

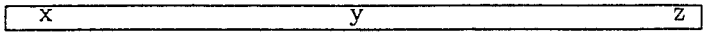

Solution 1			
r	3.09...	9.70...	14.5...
s	8.835	11.2...	13.7...
t	7.48...	6.00...	16.3...
Solution 2			
r	5.94...	8.05...	14.7...
s	8.835	3.51...	17.3...
t	11.8...	8.50...	15.8...
Solution 3			
r	9.08...	6.24...	13.9...
s	8.835	12.1...	12.9...
t	13.8...	9.69...	15.0...
Solution 4			
r	8.97...	6.31...	14.0...
s	8.835	1.53...	17.6...
t	3.71...	3.83...	15.5...

Solution 5

r	11.1...	5.02...	12.8...
s	8.835	10.3...	14.3...
t	6.19...	5.26...	16.2...

Solution 6

r	12.3...	4.38...	12.0...
s	8.835	5.54...	16.8...
t	13.2...	9.33...	15.3...

Solution 7

r	0.787...+ i 0.282...	11.03...− i 0.163...	13.9...+ i 0.113...
s	8.835	11.79...+ i 4.01...	14.2...− i 3.33...
t	4.35...+ i 4.84...	4.20...+ i 2.79...	16.7...+ i 1.50...

Solution 8

r	0.782... − i 0.282...	11.0...+ i 0.163...	13.9...− i 0.113...
s	8.835	11.7...− i 4.01...	14.2...+ i 3.33...
t	4.35...− i 4.84...	4.20...− i 2.79...	16.7...− i 1.50...

FIGURES

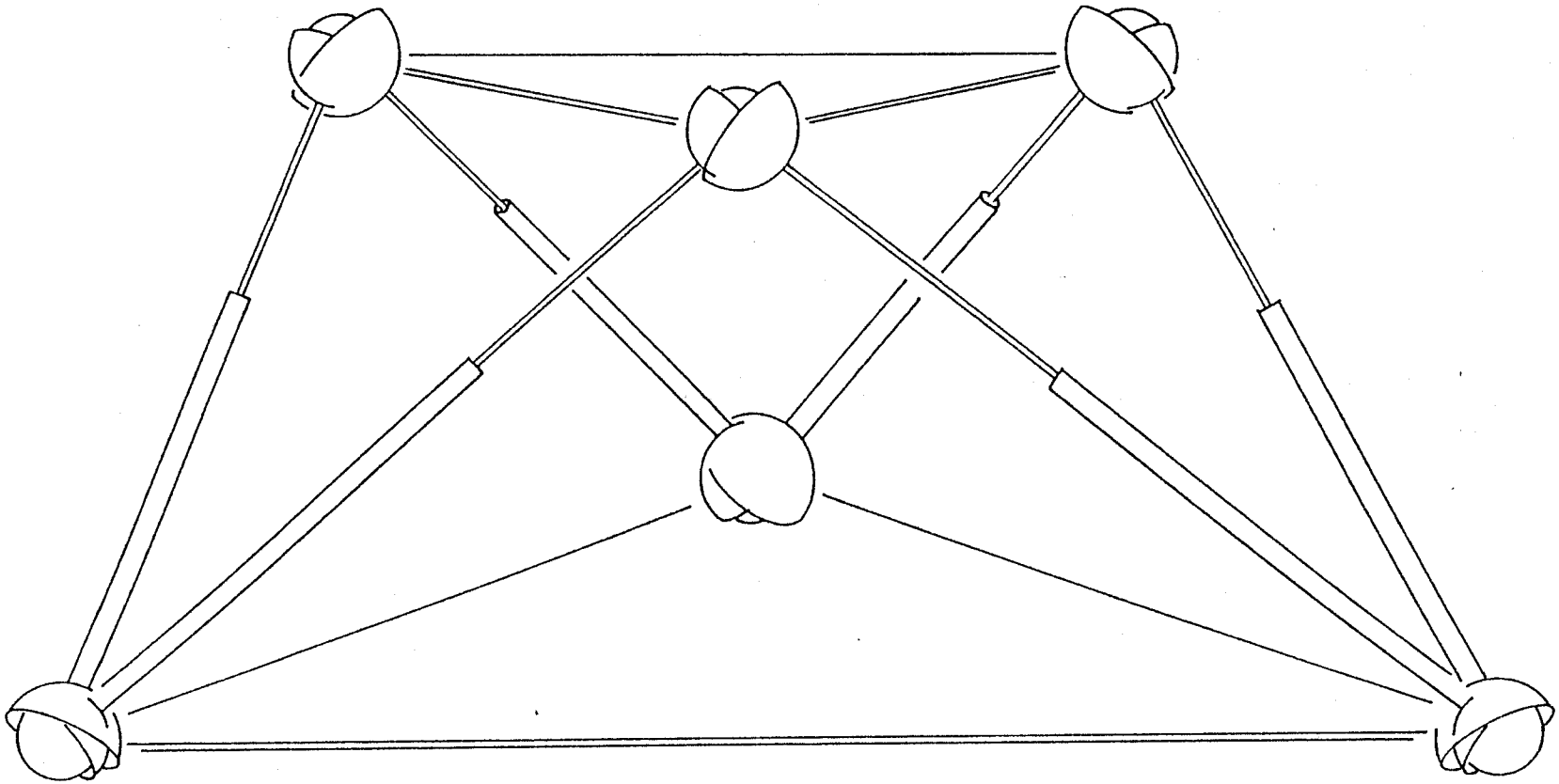

Figure 1a. The 3-3 Stewart Platform

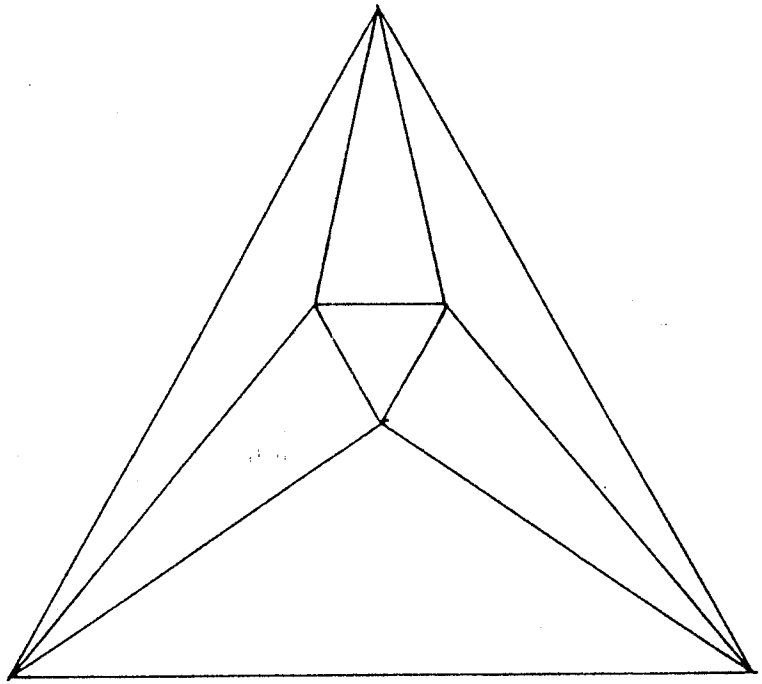

Figure 1b. The 3-3 Stewart Platform, plan view

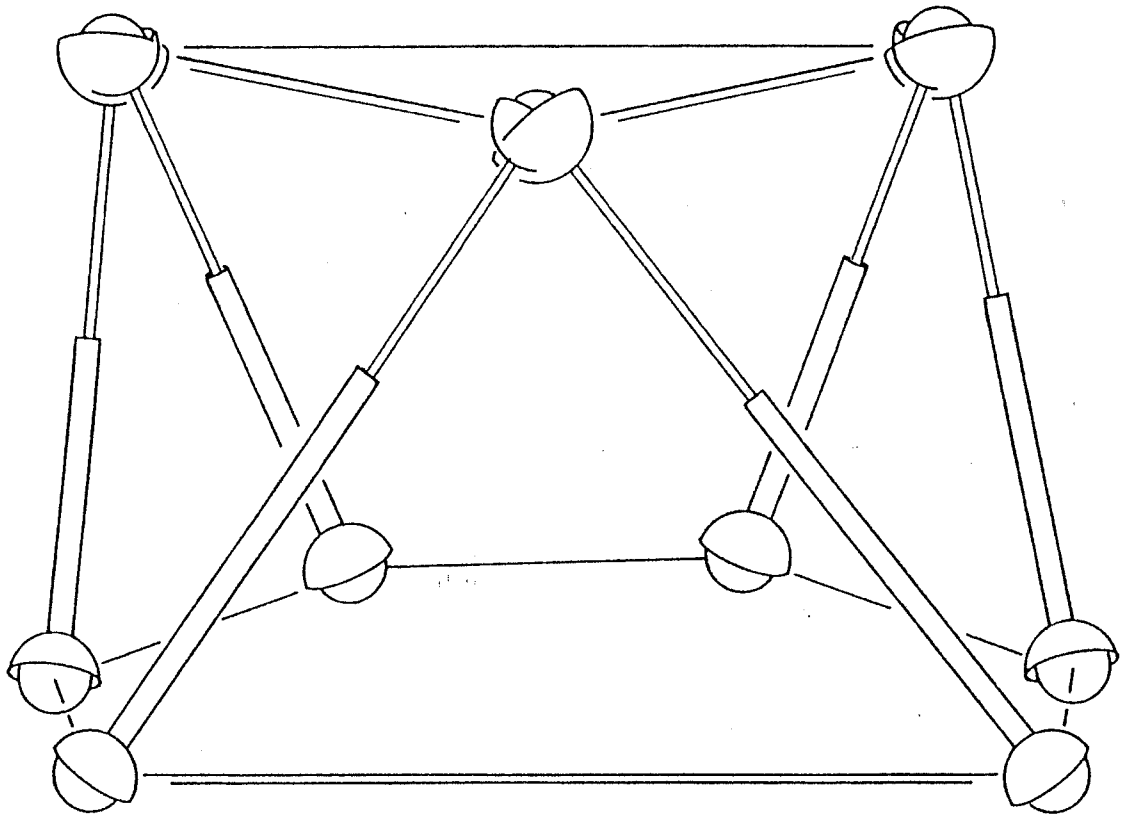

Figure 2a. The 6-3 Stewart Platform

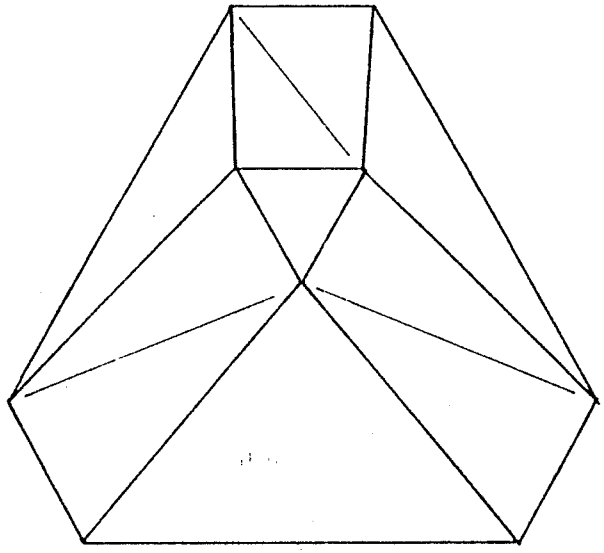

Figure 2b. The 6-3 Stewart Platform, plan view

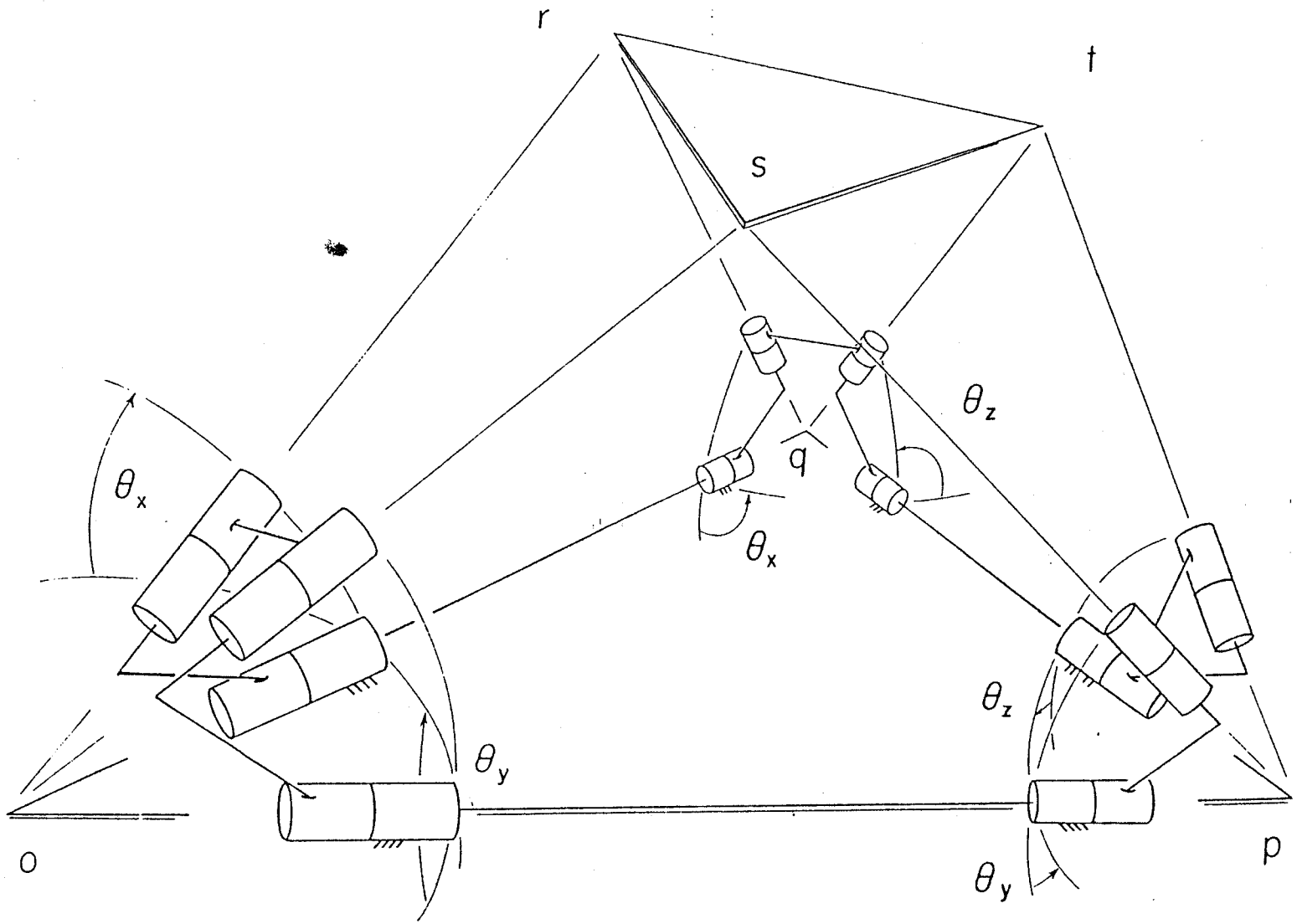

Figure 3. Three Spherical Four-Bar Mechanisms

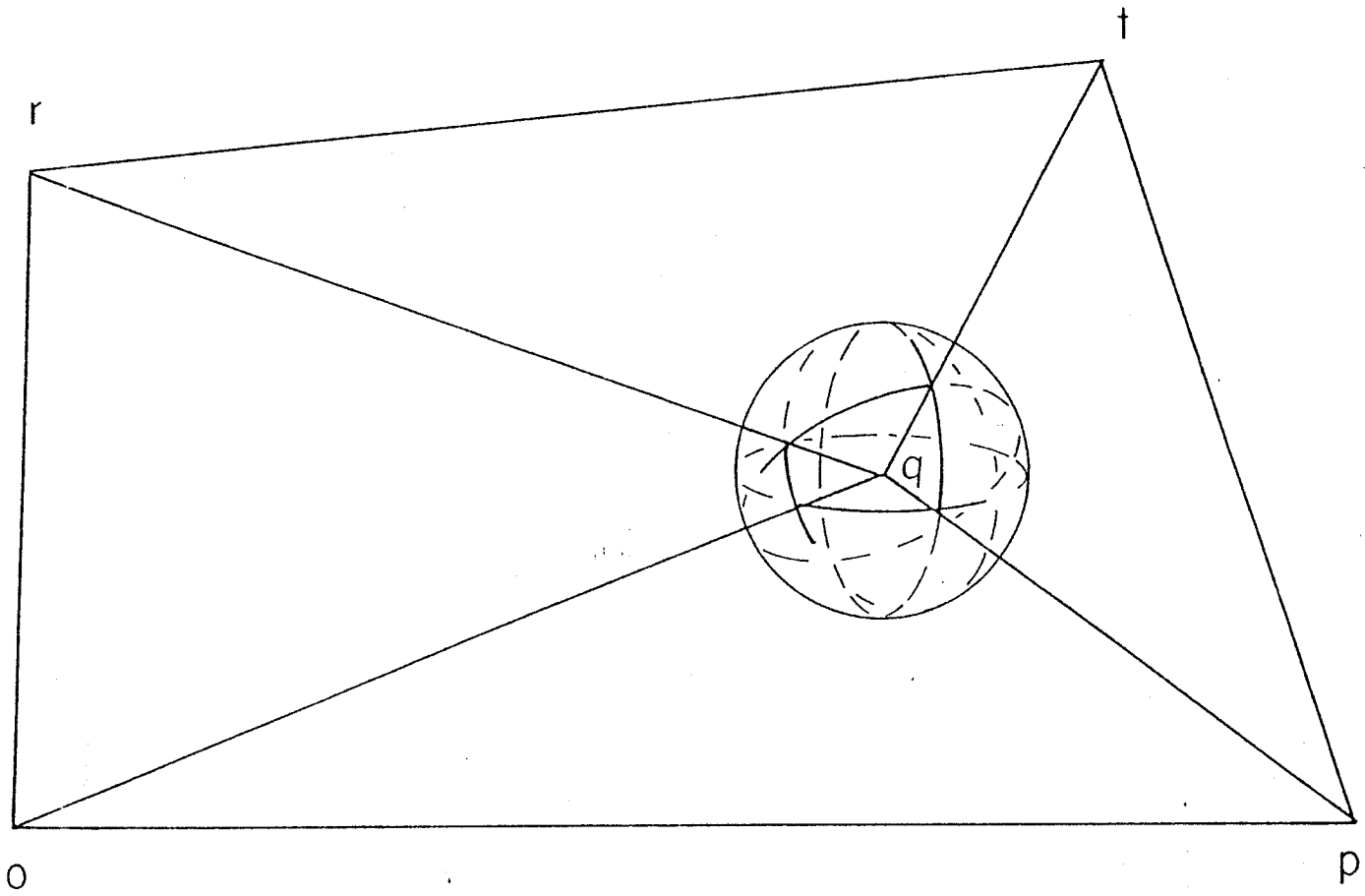

Figure 4. A Unit Sphere Located at q

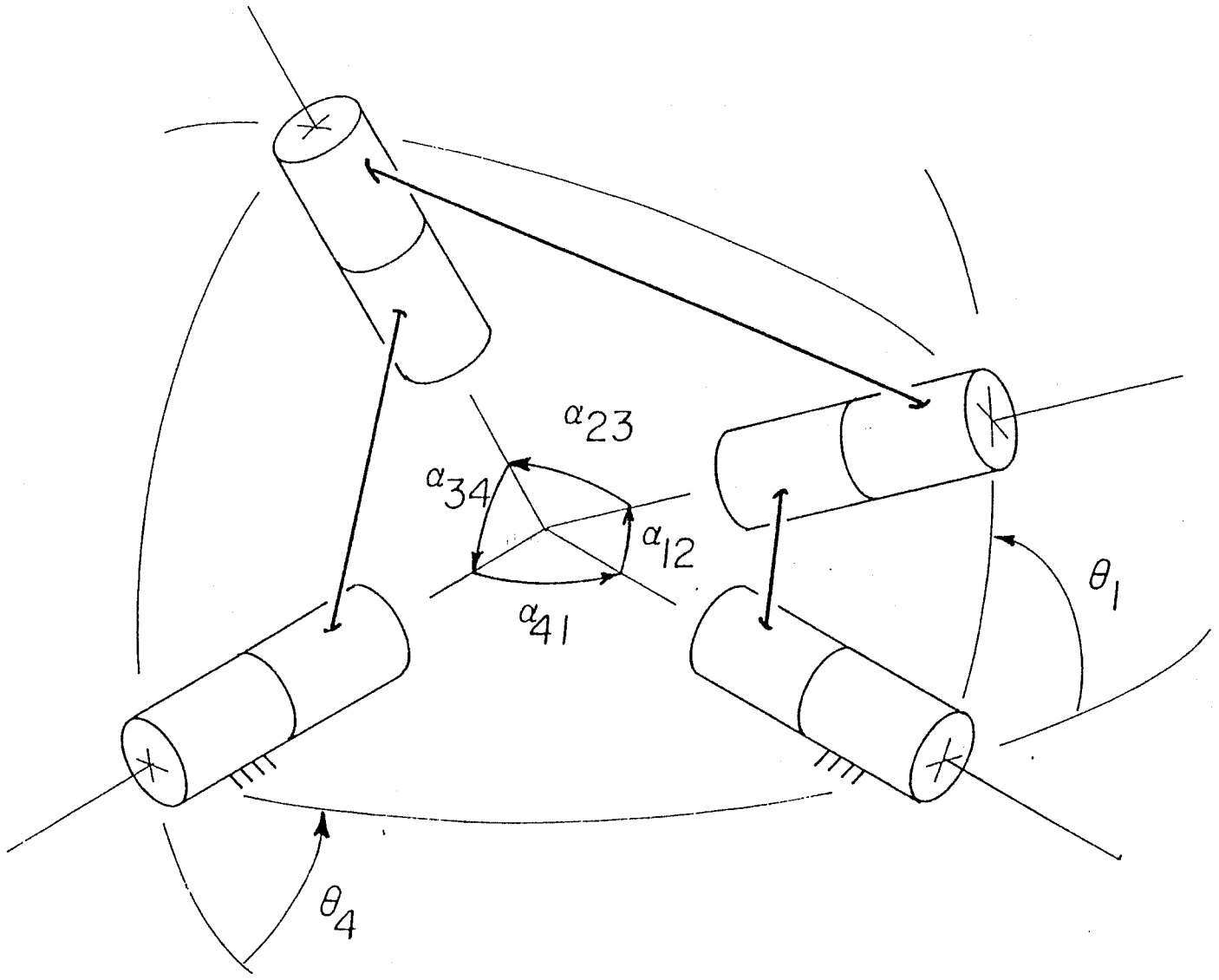

Figure 5. The generalized Spherical Four-Bar Mechanism

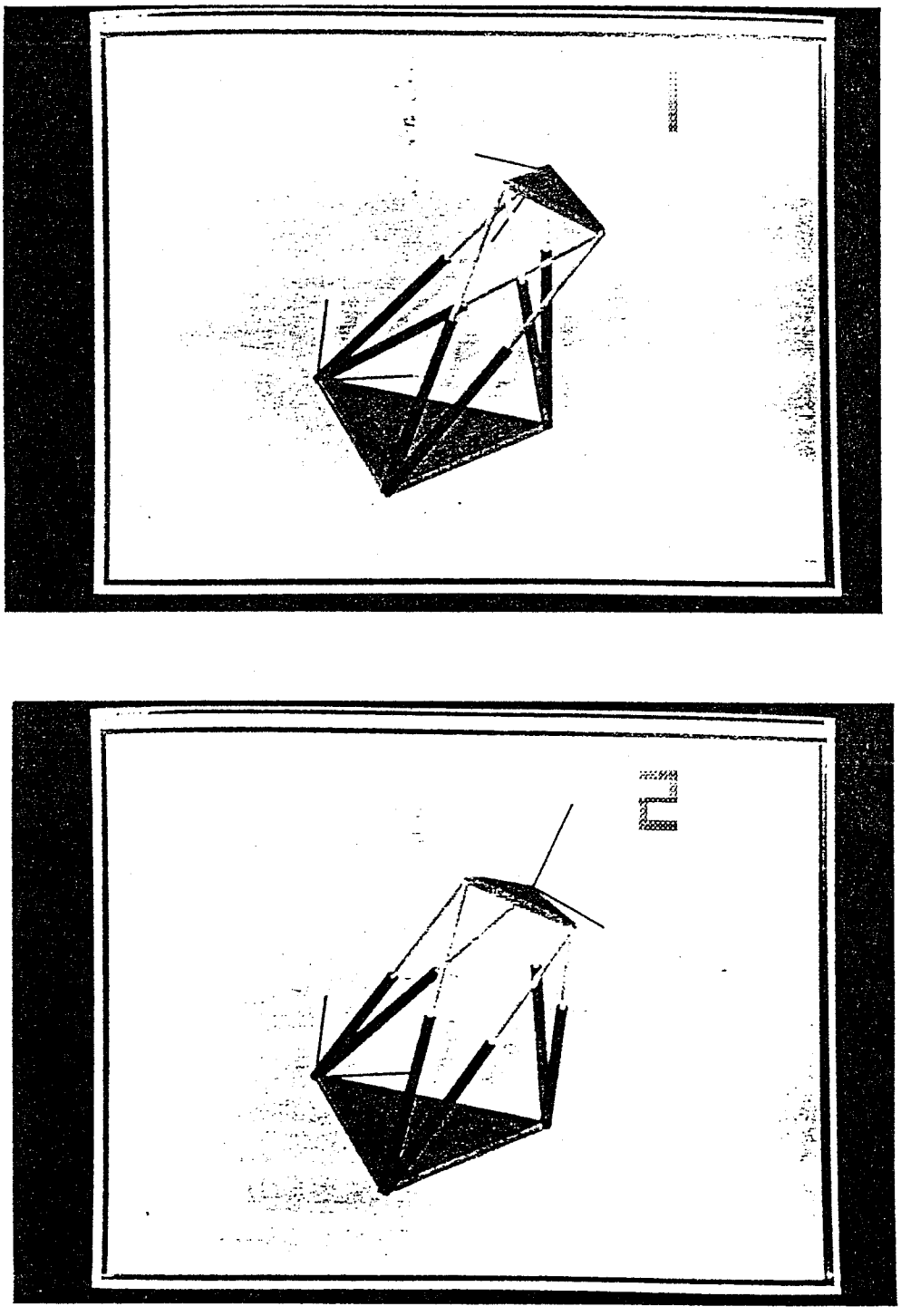

Figure 6. Six Real Solutions to the Numerical Example

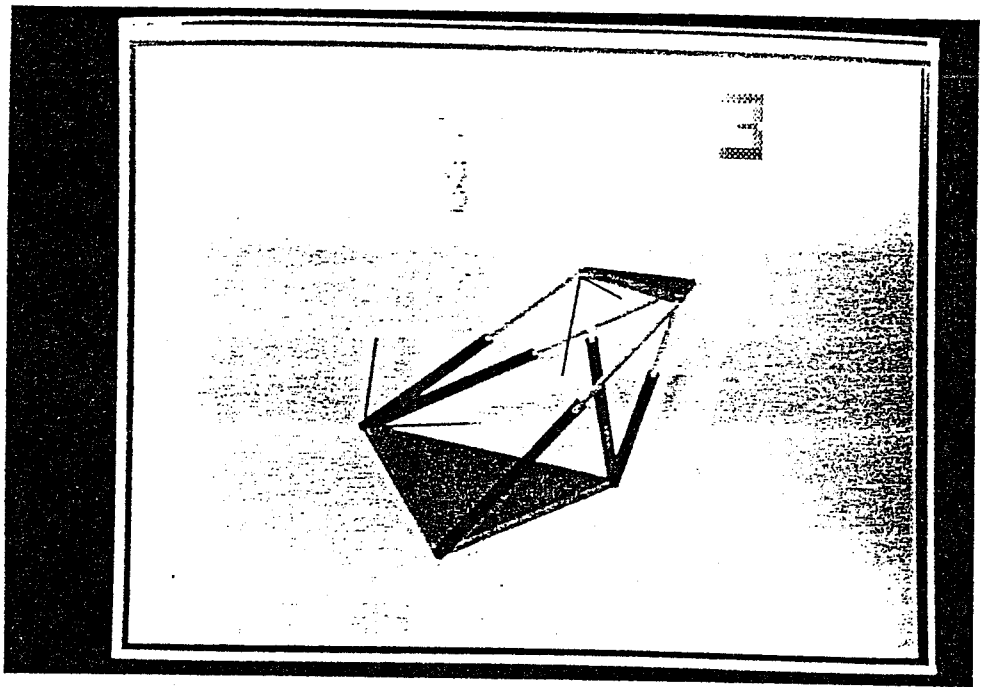

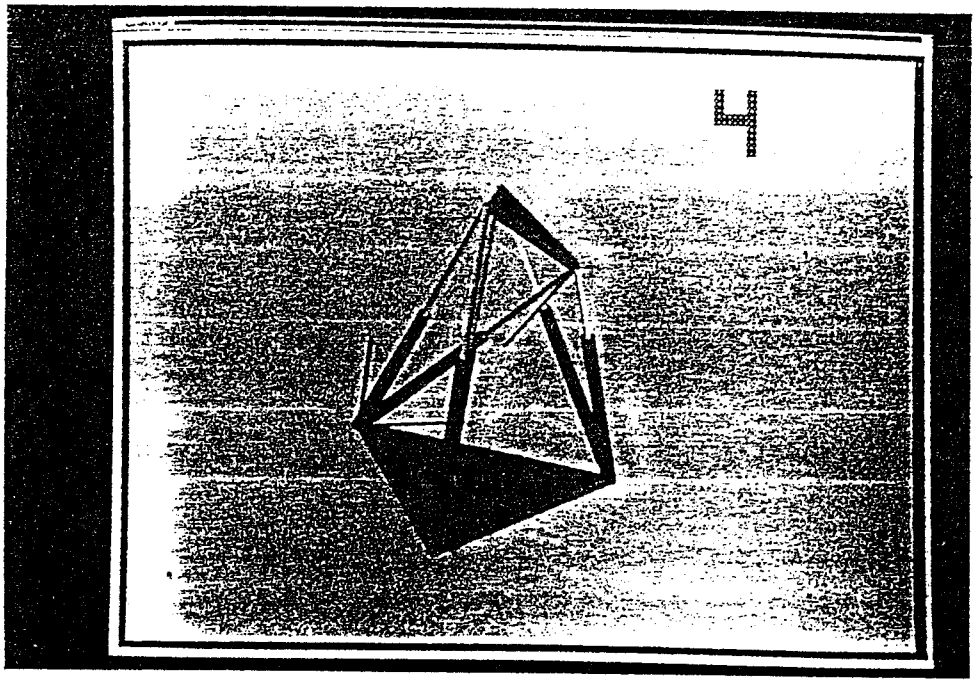

Figure 6. Six Real Solutions to the Numerical Example (Cont'd.)

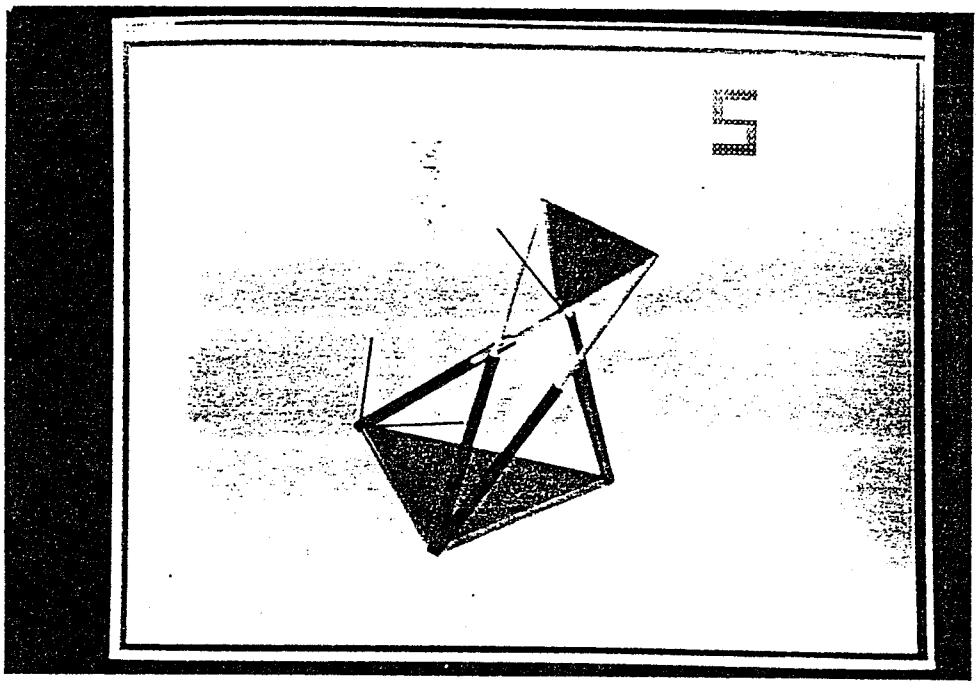

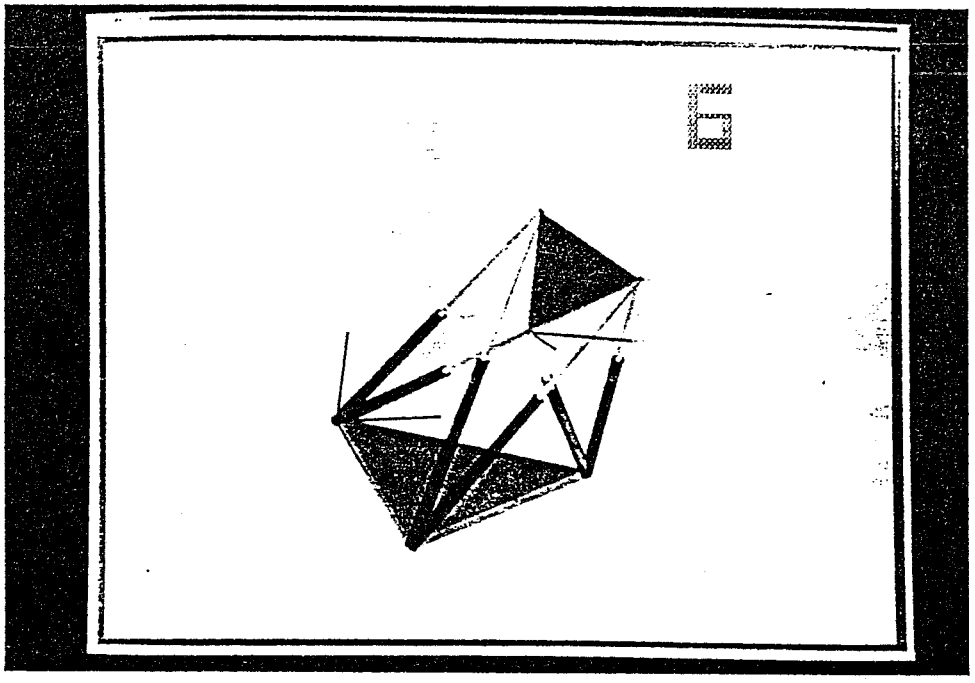

Figure 6. Six Real Solutions to the Numerical Example (Cont'd.)

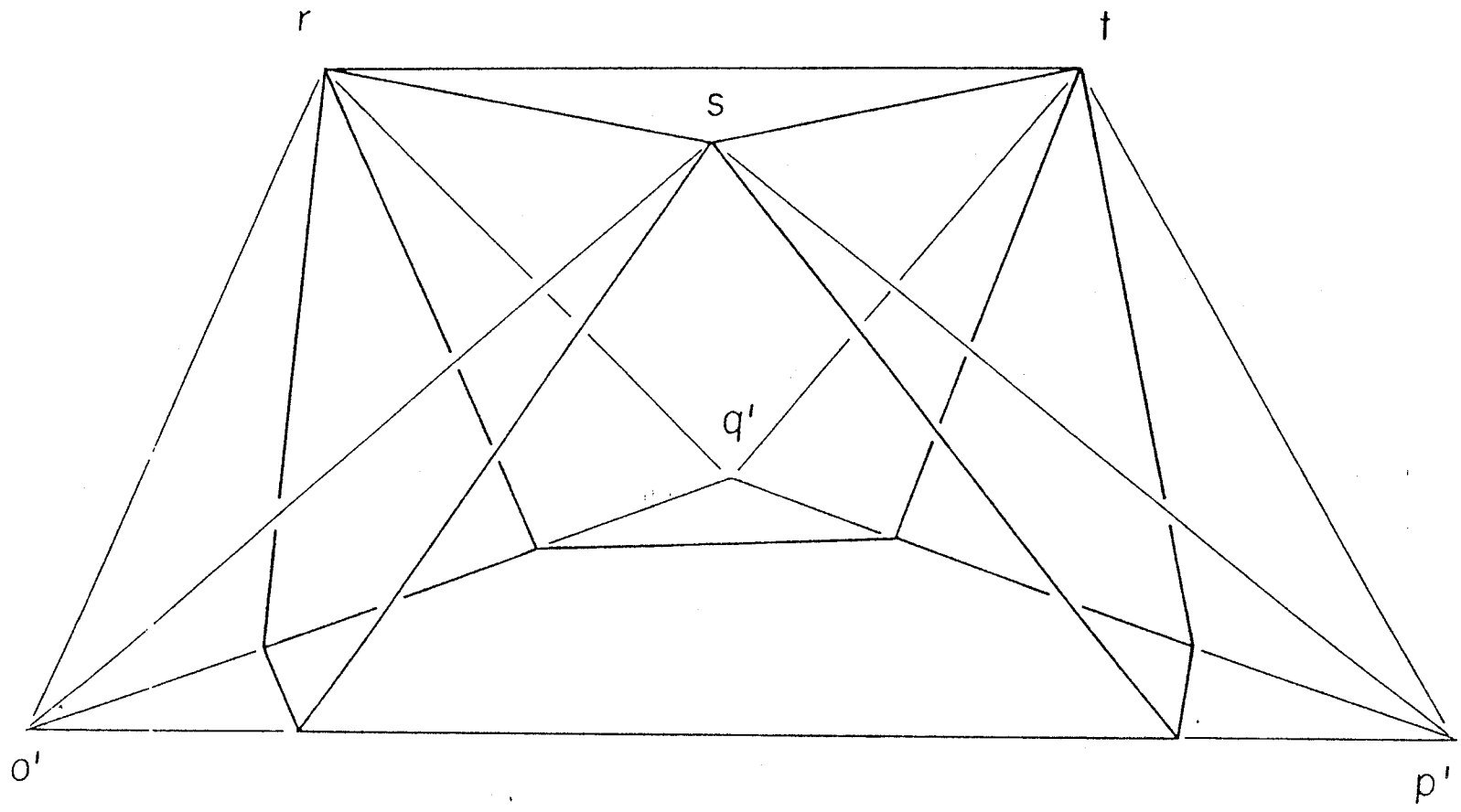

Figure 7. Constructions For The 6-3 Stewart Platform